

## Dynamic behaviors of controllably buckled thin films

Yong Wang and Xue Feng<sup>a)</sup>

AML, Department of Engineering Mechanics, Tsinghua University, Beijing 100084, People's Republic of China

(Received 29 September 2009; accepted 9 November 2009; published online 11 December 2009)

The controlled buckling of thin films is essential in the stretchable and curvilinear electronics. Through the rigorous governing equations accounting for geometric nonlinearity, dynamic behaviors of buckled thin films, which serve as interconnects in curvilinear electronics, are investigated in detail. The surface effects from surface elasticity and residual surface stress are taken into account due to the thin films thickness at small scale, and the effects of surface properties on dynamic behaviors are obtained. The results will guide the design of interconnects to avoid resonance in complicated noise environment. © 2009 American Institute of Physics.

[doi:10.1063/1.3273385]

Buckling and other mechanical instabilities usually mean loss of the carrying capacity of the structures and induce catastrophic failure. Through detailed understanding of the phenomena, however, they can provide useful tools in many applications such as microfabrication/nanofabrication,<sup>1,2</sup> bioengineering,<sup>3,4</sup> and advanced metrology methods.<sup>5,6</sup> Recently, some innovative strategies inspired by these phenomena have been proposed to improve the stretchability of electronic devices and to fit the curvilinear layouts.<sup>7–11</sup> The most promising way is to use buckled thin films, which serve as interconnects, to link electronic components on isolated rigid islands,<sup>10,11</sup> as shown in Fig. 1(a). One of the important advantages of this way is that the buckled geometries of thin films can be precisely controlled by prestrain, and so the stretchability can be designed. Energy method has been performed to obtain the buckled amplitude and maximum strain of thin film for given prestrain, and these conclusions guide the design of interconnects to avoid fracture.<sup>10,11</sup> As electronic devices, however, the circuits will eventually work in complicated noise environment and undergo stochastic disturbances including mechanical, electric, and thermal loading. So, strength consideration is not enough and the dynamic behaviors of buckled thin films should be analyzed to guide the design of interconnects to avoid resonance in operating conditions.

Moreover, surface energy could be significant enough to compete with the strain energy for ultrathin films with thickness at submicron or nanometer scale. A simple comparison between typical surface energy density of solids ( $\approx 1 \text{ J/m}^2$ ) and strain energy density ( $\approx 10^7 \text{ J/m}^3$ ) suggests that surface energy could become important for film thickness in the order of 100 nm ( $10^{-7} \text{ m}$ ) or less.<sup>12</sup> Many attempts have been made to reveal the influence of surface properties on elastic properties of nanobeams, nanowires, nanoplates, etc.<sup>13–16</sup> The thickness of thin films serving as interconnects is at submicron scale (about 50 nm),<sup>10,11</sup> and so the surface effects on its mechanical behaviors should be considered.

The width of thin film (i.e., interconnects) is much smaller than the width of island such that the rotation at the

ends of thin film is very small. So, the thin film can be modeled as beam fixed at two ends.<sup>11</sup> The initial and final distance in adjacent islands is  $l_0$  and  $l$ , respectively [shown in Fig. 1(b)]. The rectangular section of thin film has width  $b$  and thickness  $h$  [shown in Fig. 1(c)]. The Young's modulus of bulk and surface layer are  $E$  and  $E_1$ , and the thickness of surface layer is  $t$ . Adopting the surface-layer-based model<sup>16</sup> and neglecting the effect of lateral sides ( $b \gg h$ ), the effective tension stiffness and bending stiffness induced by surface elasticity are  $EA^* \approx EA(1 + \alpha)$ ,  $EI^* \approx EI(1 + 3\alpha)$ , in which  $A = bh$ ,  $I = bh^3/12$ ,  $\alpha = 2E_s/(Eh)$ , and  $E_s = E_1t$ .  $\alpha$  is nondimensional surface elasticity. Residual surface stress can be replaced by an effective distributed loading on the upper surface  $\hat{q}(\hat{x}, \hat{t}) = 2\tau^0 b \partial^2 \hat{w} / \partial \hat{x}^2$ , where  $\hat{w}$  is the out-plane displacement of the thin film and  $\tau^0$  is the residual surface stress when the bulk is under unstrained.<sup>16</sup>

The thin film is subject to a compressive axial force  $\hat{P}_0 = EA^* \varepsilon_0 = EA^*(1 - l/l_0)$  at flat state, where  $\varepsilon_0$  is prestrain which controls the buckled geometry. This flat state is taken as the reference configuration [shown in Fig. 1(b)]. The following nondimensional variables are introduced:  $x = \hat{x}/l$ ,  $w = \hat{w}/r$ ,  $r = \sqrt{I/A}$ ,  $t = \hat{t} \sqrt{EI/(\rho l^4)}$ ,  $P_0 = \hat{P}_0 l^2/(EI)$ , and  $P_1 = 2\tau^0 b l^2/(EI)$ , where  $w$  is nondimensional deflection,  $r$  is the radius of gyration of the cross section, and  $P_1$  is the nondimensional residual surface stress. Then, the governing equation and boundary conditions are expressed as

$$\ddot{w} + (1 + 3\alpha)w'''' + \left[ P_0 - P_1 - (1 + \alpha)(1 - \varepsilon_0) \int_0^1 w'^2 dx/2 \right] w'' = 0, \quad (1a)$$

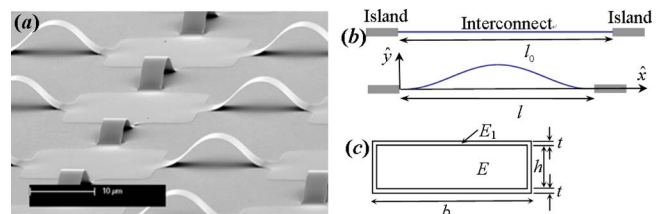


FIG. 1. (Color online) Schematic diagram of buckled thin films. (a) SEM picture of buckled films in interconnect-bridge structure (See Ref. 10); (b) After the prestrain is released, the film buckles and is modeled as beams fixed at two ends; (c) Rectangular cross section of thin films with surface layers.

<sup>a)</sup> Author to whom correspondence should be addressed. Electronic mail: fengxue@tsinghua.edu.cn.

$$w = 0, w' = 0 \quad x = 0, 1. \quad (1b)$$

The nonlinearity arises from the midplane stretching of buckled thin film.

By dropping the dynamic terms and denoting  $[P_0 - P_1 - (1 + \alpha)(1 - \varepsilon_0) \int_0^1 w'^2 dx / 2] / (1 + 3\alpha) = \lambda^2$ , Eq. (1a) reduces to a fourth-order ordinary-differential equation  $w'''' + \lambda^2 w'' = 0$ . Combining this equation and boundary condition [Eq. (1b)], the eigenvalues  $\lambda_i$  can be obtained by solving the characteristic equation and the  $i$ -th mode shape is obtained subsequently. Then, the amplitude of the  $i$ -th mode shape is determined through the relationship  $[P_0 - P_1 - (1 + \alpha)(1 - \varepsilon_0) \int_0^1 w_i'^2 dx / 2] / (1 + 3\alpha) = \lambda_i^2$ . For the buckled thin films serving as interconnects, antisymmetric mode shapes cannot appear due to the existence of compliant substrate. The first-order symmetric mode shape concerned here is  $w_1(x) = c_1[1 - \cos(\lambda_1 x)]$ , in which

$$c_1 = 2 \sqrt{\frac{1 + 3\alpha}{(1 - \varepsilon_0)(1 + \alpha)} \left\{ \frac{1}{1 + 3\alpha} \left[ (1 + \alpha) \frac{\varepsilon_0}{\varepsilon_c} - \frac{P_1}{4\pi^2} \right] - 1 \right\}}, \quad (2)$$

where  $\lambda_1 = 2\pi$ , and  $\varepsilon_c = (h/l)^2 \pi^2 / 3$  is the first-order critical buckling strain without considering surface effects. The amplitude  $c_1$  of buckled configuration depends on surface elasticity  $\alpha$ , residual surface stress  $P_1$  and prestrain  $\varepsilon_0$ .

The effect of surface properties on critical compression of buckling obtained from Eq. (2) is  $\hat{P}_0^{cr} / (4\pi^2 EI / l^2) = 1 + 3\alpha + (l/h)^2 6\tau_0 / (\pi^2 Eh)$ , which is consistent with the result through the method in Ref. 16. Neglecting the effects of surface properties, the first-order mode shape obtained here supports the result in Refs. 10 and 11. In these references, the postbuckling configuration is obtained by assuming a mode shape and minimizing the system energy, and so its accuracy is dependent on the assumption of this mode shape. The postbuckling configuration obtained here, however, is based on the rigorous governing equations and is the analytic solution.

Now let  $v(x, t) = w(x, t) - w_1(x)$ , where  $v(x, t)$  is a small dynamic disturbance around first-order buckled configuration  $w_1(x)$ . Substitution of it into Eq. (1a) yields the governing equation with respect to disturbance  $v(x, t)$ . With the condition of  $v \ll w_1$ , high-order terms of  $v$  can be ignored.<sup>17</sup> Then the simplified governing equation and corresponding boundary conditions are

$$\begin{aligned} \ddot{v} + (1 + 3\alpha)v'''' + (1 + 3\alpha)\lambda_1^2 v'' \\ = (1 + \alpha)(1 - \varepsilon_0)w_1'' \int_0^1 v' w_1' dx, \end{aligned} \quad (3a)$$

$$v = 0, v' = 0 \quad x = 0, 1. \quad (3b)$$

Separating time and space variables and substituting  $v(x, t) = V(x)T(t)$  into Eq. (3) yield the following equation and boundary conditions for  $V(x)$ :

$$\begin{aligned} (1 + 3\alpha)V'''' + (1 + 3\alpha)\lambda_1^2 V'' - \omega^2 V \\ = (1 + \alpha)(1 - \varepsilon_0)w_1'' \int_0^1 V' w_1' dx, \end{aligned} \quad (4a)$$

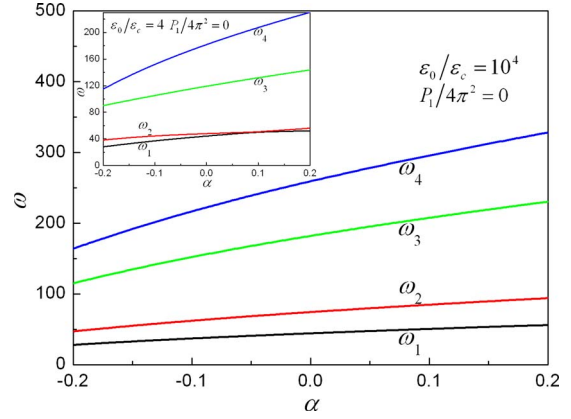


FIG. 2. (Color online) The effects of surface elasticity  $\alpha$  on nondimensional natural frequencies  $\omega$ .

$$V(0) = 0, V'(0) = 0, V(1) = 0, V'(1) = 0. \quad (4b)$$

Equation (4a) is a nonhomogeneous fourth-order ordinary-differential equation, and the general solution of which can be expressed as summation of homogeneous solution  $V_h(x)$  and particular solution  $V_p(x)$ . The homogeneous solution is  $V_h = d_1 \sin(s_1 x) + d_2 \cos(s_1 x) + d_3 \sinh(s_2 x) + d_4 \cosh(s_2 x)$ , where  $d_k (k=1, \dots, 4)$  are undetermined constants and  $s_{1,2} = \sqrt{\pm \lambda_1^2 / 2 + \sqrt{\lambda_1^4 + 4\omega^2 / (1 + 3\alpha)} / 2}$ . The particular solution satisfies the following equation:

$$\begin{aligned} (1 + 3\alpha)V_p'''' + (1 + 3\alpha)\lambda_1^2 V_p'' - \omega^2 V_p \\ = (1 + \alpha)(1 - \varepsilon_0)w_1'' \int_0^1 (V_h' + V_p')w_1' dx. \end{aligned} \quad (5)$$

Substitution of particular solution  $V_p = d_5 w_1''$  into Eq. (5) obtains the relationship between  $d_5$  and  $d_k (k=1, \dots, 4)$

$$\begin{aligned} [\omega^2 - (1 + \alpha)(1 - \varepsilon_0)c_1^2 \lambda_1^4 / 2] d_5 \\ + (1 + \alpha)(1 - \varepsilon_0) \int_0^1 V_h' w_1' dx = 0 \end{aligned} \quad (6)$$

Inserting the general solution  $V_h + V_p$  into the boundary conditions [Eq. (4b)] yields four equations, which combining with Eq. (6) constitute a system of five homogeneous algebraic equations for constants  $d_5$  and  $d_k (k=1, \dots, 4)$ . Solution of this eigenvalue problem produces nondimensional natural frequencies  $\omega_i$ .

In the following discussion, we take the initial flat state as reference configuration. Two cases are discussed simultaneously. One is the case of curvilinear electronics in which buckled films serve as interconnects with the large ratio of  $\varepsilon_0 / \varepsilon_c$  usually ranging within  $[10^2, 10^7]$ .<sup>10,11</sup> The other is the case of initial buckling with the small ratio of  $\varepsilon_0 / \varepsilon_c$  ranging within  $[1, 10]$ .

The effects of surface elasticity  $\alpha$  on nondimensional natural frequencies  $\omega_i$  are shown in Fig. 2.  $\omega_i$  increases prominently with increase of surface elasticity in two cases. The effects of residual surface stress  $P_1$  on  $\omega_i$  for the case of initial buckling are shown in Fig. 3. It is found that  $\omega_1$  and  $\omega_4$  hold constant and  $\omega_2$  and  $\omega_3$  decrease as  $P_1$  increases.  $\omega_1$  and  $\omega_2$  will switch each other if  $P_1$  increases further. Furthermore, the buckled thin films will enter the planar configuration when  $P_1$  approaches a certain positive value (about  $12\pi^2$  at present).

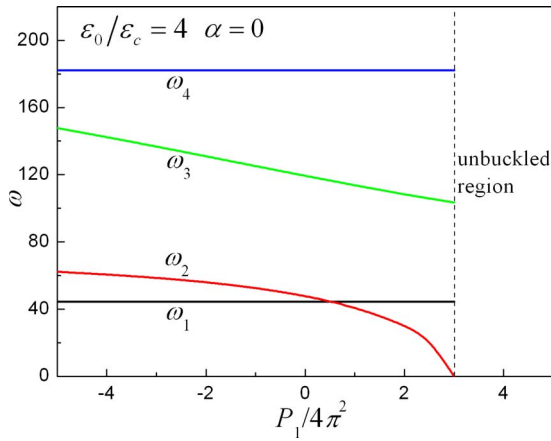


FIG. 3. (Color online) The effects of residual surface stress  $P_1/(4\pi^2)$  on nondimensional natural frequencies  $\omega$ .

Results for nondimensional natural frequencies  $\omega_i = \Omega_i/(\sqrt{E/(12\rho_0)h/l_0^2})$  versus ratio of  $\varepsilon_0/\varepsilon_c$  accounting for surface elasticity are shown in Fig. 4. For the case of initial buckling, some  $\omega_i$  hold constant but others increase as prestrain  $\varepsilon_0/\varepsilon_c$  increases.<sup>17</sup> For the case in curvilinear electronics, all of nondimensional natural frequencies  $\omega_i$  almost hold constant with the ratio of  $\varepsilon_0/\varepsilon_c$  varying in wide range for given  $\alpha$  (refer to inset in Fig. 4). Equation (2) shows that the effect of residual surface stress  $P_1/4\pi^2$  is equivalent to that of  $\varepsilon_0/\varepsilon_c$  and variation of  $P_1/4\pi^2$  corresponds to that of  $\varepsilon_0/\varepsilon_c$ . Then the nondimensional natural frequencies  $\omega_i$  will also hold constant if the residual surface stress  $P_1/4\pi^2$  varies. For given prestrain  $\varepsilon_0 \in [0.02, 0.20]$  and different  $l_0/h \in [200, 5000]$ ,  $\varepsilon_0/\varepsilon_c = \varepsilon_0(l_0/h)^2/3/\pi^2 \in [10^2, 10^7]$  and  $\omega_i$  hold constants, but natural frequencies

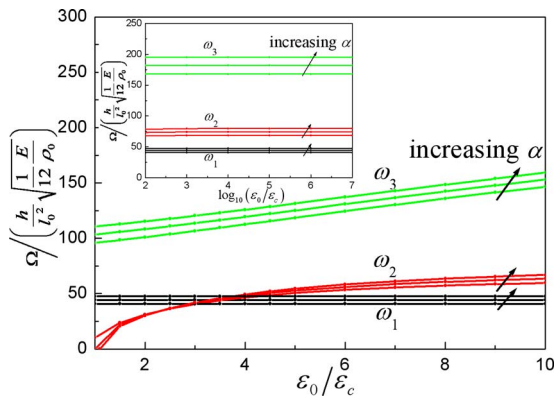


FIG. 4. (Color online) Nondimensional natural frequencies  $\omega$  vs the ratio of  $\varepsilon_0/\varepsilon_c$ . The lowest three natural frequencies are shown and each contains surface elasticity  $\alpha = -0.05, 0$ , and  $0.05$ , respectively.

$\Omega_i = \omega_i(\sqrt{E/(12\rho_0)h/l_0^2})$  vary in a wide range. This means that natural frequencies  $\Omega_i$  of interconnects can be designed by selecting  $h$  and  $l_0$  properly to keep it away from external frequencies. Fixed the value of height  $h$ , for instance, natural frequencies  $\Omega_i$  can be tune in two magnitude by selecting the value of length  $l_0$  in one magnitude. Clearly,  $\Omega_i$  will be tuned in a wider range if height  $h$  is also a designable parameter. For given  $h$  and  $l_0$ , the variation of prestrain  $\varepsilon_0$  in interval  $[0.02, 0.20]$  will not affect  $\Omega_i$ . Therefore, the natural frequencies  $\Omega_i$  will keep constant when the ‘interconnect-island’ structure is stretched or compressed. The important significance of this characteristic is that the structure will not resonate when stretching or compressing if natural frequencies  $\Omega_i$  are designed to keep away from external frequencies.

In summary, the dynamic behaviors of buckled thin films are analyzed and the effects of surface properties are taken into account, which tries to fundamentally understand controlled buckling behavior of thin films.

We gratefully acknowledge the support from National Natural Science Foundation of China (Grant Nos. 10820101048, 10832005, and 90816007) and Foundation for the Author of National Excellent Doctoral Dissertation of China (FANEDD) (Grant No. 2007B30).

<sup>1</sup>N. Bowden, S. Brittain, A. G. Evans, J. W. Hutchinson, and G. M. Whitesides, *Nature (London)* **393**, 146 (1998).

<sup>2</sup>N. Bowden, W. T. S. Huck, K. E. Paul, and G. M. Whitesides, *Appl. Phys. Lett.* **75**, 2557 (1999).

<sup>3</sup>A. K. Harris, P. Wild, and D. Stopak, *Science* **208**, 177 (1980).

<sup>4</sup>X. Jiang, S. Takayama, X. Qian, E. Ostuni, H. Wu, N. Bowden, P. LeDuc, D. E. Ingber, and G. M. Whitesides, *Langmuir* **18**, 3273 (2002).

<sup>5</sup>C. M. Stafford, C. Harrison, K. L. Beers, A. Karim, E. J. Amis, M. R. Vanlandingham, H.-C. Kim, W. Volksen, R. D. Miller, and E. E. Simonyi, *Nature Mater.* **3**, 545 (2004).

<sup>6</sup>E. A. Wilder, S. Guo, S. Lin-Gibson, M. J. Faselka, and C. M. Stafford, *Macromolecules* **39**, 4138 (2006).

<sup>7</sup>D.-Y. Khang, H. Jiang, Y. Huang, and J. A. Rogers, *Science* **311**, 208 (2006).

<sup>8</sup>H. Jiang, Y. Sun, J. A. Rogers, and Y. Huang, *Appl. Phys. Lett.* **90**, 133119 (2007).

<sup>9</sup>S. P. Lacour, J. Jones, S. Wagner, and Z. Suo, *Proc. IEEE* **93**, 1459 (2005).

<sup>10</sup>H. C. Ko, M. P. Stoykovich, J. Song, V. Malyarchuk, W. M. Choi, C.-J. Yu, J. B. Geddes III, J. Xiao, S. Wang, Y. Huang, and J. A. Rogers, *Nature (London)* **454**, 748 (2008).

<sup>11</sup>J. Song, Y. Huang, J. Xiao, S. Wang, K. C. Kwang, H. C. Ko, D.-H. Kim, M. P. Stoykovich, and J. A. Rogers, *J. Appl. Phys.* **105**, 123516 (2009).

<sup>12</sup>R. Huang, C. M. Stafford, and B. D. Vogt, *J. Aerosp. Eng.* **20**, 38 (2007).

<sup>13</sup>J. Lagowski, H. C. Gatos, and E. S. Sproles, *Appl. Phys. Lett.* **26**, 493 (1975).

<sup>14</sup>M. E. Gurtin, X. Markenscoff, and R. N. Thurston, *Appl. Phys. Lett.* **29**, 529 (1976).

<sup>15</sup>M. J. Lachut and J. E. Sader, *Phys. Rev. Lett.* **99**, 206102 (2007).

<sup>16</sup>G. F. Wang and X. Q. Feng, *Appl. Phys. Lett.* **94**, 141913 (2009).

<sup>17</sup>A. H. Nayfeh and S. A. Emam, *Nonlinear Dyn.* **54**, 395 (2008).